Available online at www.sciencedirect.com
ScienceDirect
Energy Reports 8 (2022) 989–998
www.elsevier.com/locate/egyr

2022 International Conference on Energy Storage Technology and Power Systems (ESPS 2022), February 25–27, 2022, Guilin, China

Power yield improvement of wind turbine and fatigue load mitigation using predictive-based Active flow controller

G. Srinivasa Sudharsan[a], R. Venkatasubramanian[b], N. Hemalatha[c], Radhika G. Deshmukh[d], Mohana Alanazi[e], Ahmad Almadhor[f], S. Lokesh[g], Karthikeyan N.[h,*], M. Sudhakar[i]

[a] *Department of Electronics and Communication Engineering, Vel Tech Rangarajan Dr. Sagunthala R&D Institute of Science and Technology, Avadi, Chennai, Tamil Nadu 600062, India*
[b] *Department of Electrical and Electronics Engineering, New Prince Shri Bhavani College of Engineering and Technology, Chennai 600073, Tamil Nadu, India*
[c] *Department of Electronics and Communication Engineering, Saveetha School of Engineering, Saveetha Institute of Medical And Technical Sciences, Chennai, Tamil Nadu 600124, India*
[d] *Department of Physics, Shri Shivaji Science College Amravati, Maharashtra 444603, India*
[e] *Department of Electrical Engineering, College of Engineering, Jouf University, Sakaka 42421, Saudi Arabia*
[f] *Department of Computer Engineering and Networks, Jouf University, Sakaka 42421, Saudi Arabia*
[g] *Department of Computer Science and Engineering, PSG Institute of Technology and Applied Research, Coimbatore 641062, Tamil Nadu, India*
[h] *Department of Mechanical Engineering, National Institute of Technology, Tiruchirappalli 620015, India*
[i] *Department of Mechanical Engineering, Sri Sai Ram Engineering College, Chennai 600044, Tamil Nadu, India*

Received 4 October 2022; accepted 10 October 2022
Available online 28 October 2022

Abstract

The wind turbine construction aging caused by fatigue components of a wind field over a long period affects the physical structure. Flow controlling methodologies are used to alleviate turbine assembly stress. The flow regulation approach controller is critical in the fatigue load minimization procedure. This paper offers a Predictive controller for Independent pitch control (IPC)-based flow management. Because of the azimuthal position of the blade, the flow dynamics of the blades are vulnerable to cyclic fluctuations. This paper considers the azimuthal angle blade dynamics since there is a significant variation in movements between the bottom and top blades. The suggested controller (which takes into account the wind turbine's Azimuthal angle characteristics) outperforms the existing controllers in terms of its capacity to forecast the blade's reaction as it approaches the azimuthal location. The complete replication was effectively done.

Peer-review under responsibility of the scientific committee of the International Conference on Energy Storage Technology and Power Systems ESPS 2022.

Keywords: Azimuthal angle; Active flow control; Damage equivalent load

* Corresponding author.
E-mail address: rsskarthikeyan@gmail.com (Karthikeyan N.).

https://doi.org/10.1016/j.egyr.2022.10.285

Peer-review under responsibility of the scientific committee of the International Conference on Energy Storage Technology and Power Systems ESPS 2022.

1. Introduction

The rise in wind turbine configuration achieves the rapid development of wind energy output to fulfill the worldwide renewable energy requirements [1]. The modern dimension of a wind turbine a few years back was in kilowatts (kW), while the usual grade in the present situation is in megawatts (MWs). The rise in demand necessitates an improvement in turbine configuration as the energy output improves and the expense of energy generation decreases. However, the negative element of enlarging the wind turbine scale is that it causes challenges with fatigue load regulation of turbine construction [2]. The fatigue load of a wind turbine is caused by wasteful inclinations of wind flow striking the turbine rotor at an inclination that reduces the mechanical longevity of the wind turbine. The structure is infused with impetuous frequencies, which causes stabilization concerns in the multilayered structure [3]. The fatigue stress infringing on the internal parts, particularly the blades and the tower, must be rectified because it involves approximately 70% of the total expenditure [4].

The AFC approach modifies the pattern surrounding turbine blades by modifying the exposed area of the blade framework. Pitching is the twisting of the blade attempting to change the aerodynamic contour. The tilting alters the blade breadth open to the wind movement, allowing the wasteful portion of the wind stream to be disregarded [5]. In [6] W. Zhang et al. outlined a flow control using flaps on the wind turbine blade, and Andersen P.B et al. [7] proposed an adaptive controller for irregular periphery waves.

Pitch control might be accomplished by conducting a combined regulating operation on all of the blades in the rotor configuration. However, the dynamics of the blades differ. As a result, individualized pitch control is offered. The true effectiveness of Active flow control approaches (AFC) is held by the most optimum and suitable regulatory activity [8].

The researchers presented a Model predictive controller for navigating the IPC system using azimuthal angle-based blade variables in this paper. The root bending moment (flap and edgewise), as well as blade torsional stress, are the 2 main significant dynamic metrics to consider. The torsional stress of the blade architecture caused by wind in the z orientation causes a twisting moment in the blade framework that, if continued, would harm it. The blade root bending moment has an important influence on the operational duration of turbine constructions. As a result, the goal of this study is to minimize the preceding factors utilizing model predictive controller-based IPC management while considering the dynamics concerning the azimuthal angle. For long-term assessment, the simulation results are confirmed using the NREL FAST program. The fatigue life study generates an evaluation of the wind turbine's lifecycle DEL (Damage Equivalent Load) when used with the suggested control scheme as well as another controller.

This manuscript is arranged in the following arrangements: Section 2 reveals the dynamic characteristics; Section 3 discusses the MPC objective function; Section 4 deals with the simulation results and their analysis; Section 5 deals with the fatigue life analysis and Section 6 makes the concluding remarks of the paper.

2. Linear wind turbine model

This is a multi-variable, multi-domain structure having several degrees of freedom (DOFs). The majority of the factors cause non-linearity in the scheme. The wind turbine is a collection of various parameters [9], which comprises the rotor blade characteristics, power train, as well as generating unit. The fatigue loads are the stress created in the turbine's wind-prone regions. The fatigue load might be dampened by intercepting the wind at inclinations that catch relatively little power.

A second-order two-mass model as depicted in Fig. 1, might be utilized to replicate the dynamic behavior of the drive train framework, including the gearbox and shafts.

$$t_R - t_{LS} = \omega_R c_R + \omega_R j_R \tag{1}$$

$$t_{SH} - t_G = \omega_g c_g + \omega_g J_g \tag{2}$$

The association of the corresponding torque numbers can be given as

$$\omega_r n_g = \omega_g \tag{3}$$

$$t_{is} = n_G t_{HS} \tag{4}$$

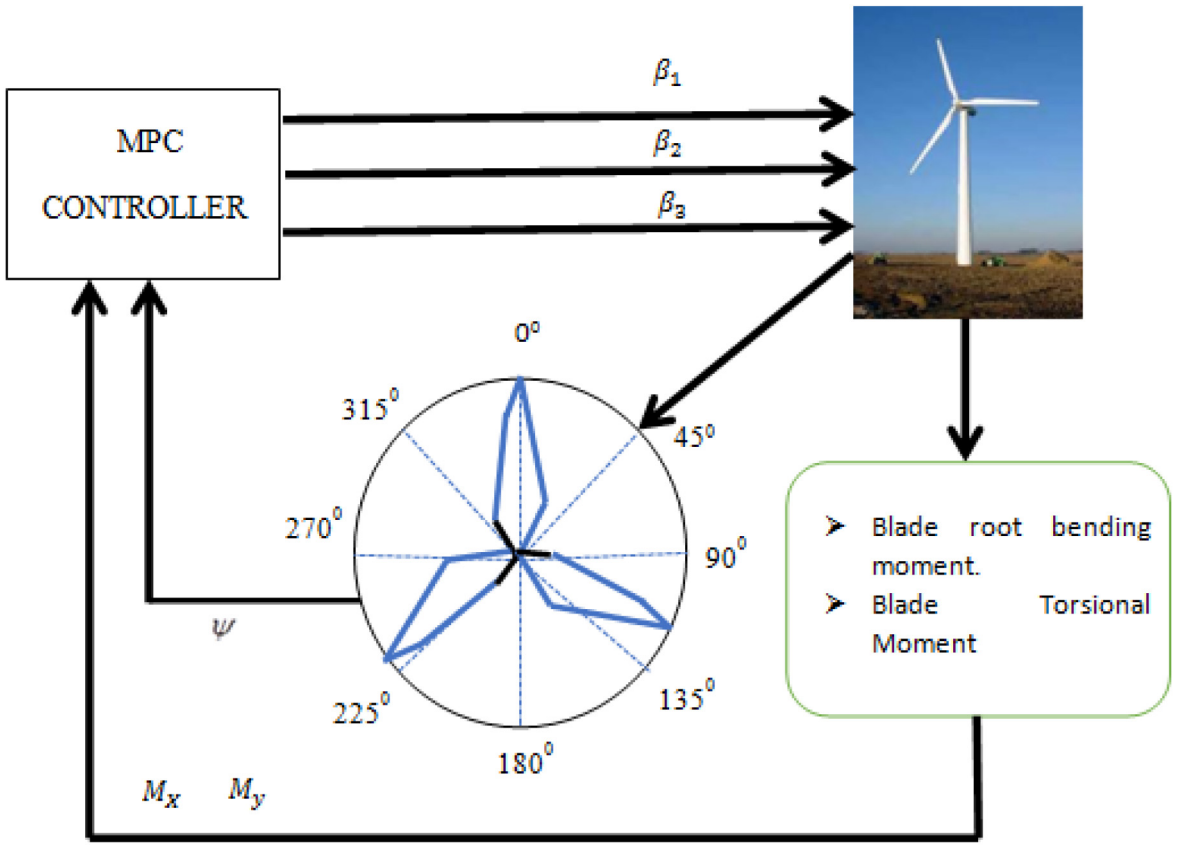

Fig. 1. Suggested control strategy Skeletal model.

The reduced speed shaft torque utilized as the fatigue load factor in this work, may be calculated using formulas (9) and (10).

$$T_{ls} = K_{ls}\left(\theta_r - \frac{\theta_g}{n_g}\right) + B_{ls}\left(\omega_r - \frac{\omega_r}{n_g}\right) \tag{5}$$

In a perfect scenario (no generator), the drive train model might be constructed from formula (3) as follows:

$$\left(C_r + n_g^2 C_g\right)\omega_r + \left(J_r + n_g^2 J_g\right)\dot{\omega_r} = T_r - n_g T_g \tag{6}$$

The speed error e is computed as given below.

$$e = \omega_r - \omega_{ref} \tag{7}$$

$$\dot{e} = \frac{T_r - n_g T_g - (C_r + n_g^2 C_g)\omega_r}{J_r + n_g^2 J_g} \tag{8}$$

The non-linear sequence is created by calculating the frequency of variation.
The tracking loop is intended to manipulate the pace of variation in generator torque, as seen beneath.

$$t_R - \left(c_R + n_G^2 C_G\right)\omega_R + \gamma\,(E)\,j_R E = n_G t_{G.REF} \tag{9}$$

The generator's electromagnetic torque demand is the primary MPPT component in any wind turbine, determining the turbine's power harvesting capability. The generator torque required influences the tip speed ratio [10]. In addition to the standard MPPT monitoring factors, fatigue load parameters and anticipatory wind information are included in the control system architecture.

3. Designing the MPC objective function

The contemporary control scheme like PID, feedback controller, etc., and optimization algorithms cannot predict the upcoming dynamics of the system [11]. But the model predictive does the anticipation of the upcoming response of the system within the prediction horizon. This estimation of the anticipated response of the system prepares the aerodynamic position of the blade when the blade is at one azimuthal position. Based on the future response the control actions are generated by the controller [12,13].

The LIDAR circuitry is used in this research to evaluate wind speed information. The LIDAR measurement is values given to the system as a measured disturbance to the multiple point Model predictive controllers (MPMPC) [14,15]. The projected wind speed information is indeed utilized to determine the MPC controller.

Horizons are another key source of anxiety; both the forecast as well as control horizons are critical. The prediction horizon N_p of the MPC should be superior to the control horizon N_c for regulating the rate of control accomplishment that establishes the consistency of the arrangement [16,17]. The formulations are synopsized further:

$$\underbrace{\begin{bmatrix} x_{k+1} \\ x_{k+2} \\ x_{k+3} \\ \vdots \\ x_{k+N_P} \end{bmatrix}}_{} = \underbrace{\begin{bmatrix} A_k \\ {A^2}_k \\ {A^3}_k \\ \vdots \\ {A^{N_P}}_k \end{bmatrix}}_{} X_K + \underbrace{\begin{bmatrix} B_k & 0 & 0 & \cdots \\ A_k B_k & B_k & 0 & \cdots \\ {A^2}_k B_k & A_k B_k & B_k & \cdots \\ \vdots & \vdots & \vdots & \vdots \\ {A^{N_P-1}}_k B_k & {A^{N_P-2}}_k B_k & {A^{N_P-3}}_k B_k & \cdots \end{bmatrix}}_{} \underbrace{\begin{bmatrix} U_k \\ U_{k+1} \\ U_{k+2} \\ \vdots \\ U_{k+N_P-1} \end{bmatrix}}_{} \tag{10}$$

$$\underbrace{\begin{bmatrix} Y_{k+1} \\ Y_{k+2} \\ Y_{k+3} \\ \vdots \\ Y_{k+N_P} \end{bmatrix}}_{} = \underbrace{\begin{bmatrix} C_k A_k \\ C_k {A^2}_k \\ C_k {A^3}_k \\ \vdots \\ C_k {A^{N_P}}_k \end{bmatrix}}_{} X_K + \underbrace{\begin{bmatrix} C_k B_k & 0 & 0 & \cdots \\ C_k A_k B_k & C_k B_k & 0 & \cdots \\ C_k {A^2}_k B_k & A_k B_k & \vdots & C_k B_k \\ \vdots & \vdots & \vdots & \vdots \\ C_k {A^{N_P-1}}_k B_k & C_k {A^{N_P-2}}_k B_k & \cdots & C_k {A^{N_P-N_u}}_k B_k \end{bmatrix}}_{} \underbrace{\begin{bmatrix} U_k \\ U_{k+1} \\ U_{k+2} \\ \vdots \\ U_{k+N_P-1} \end{bmatrix}}_{}$$

The variables are understood despite the stochastic and unpredictable nature. Therefore, state estimation is not required. The control variable of this IPC-based flow control method is the pitch angle of individual blades [18]. System stability holds a major concern on the rate of change of individual pitch angles. There should be a level of optimum change of pitch angle to be maintained. Therefore, the online recursive regulating rule is outlined using the minimization cost function J within the control horizon N_p by maintaining the Δu as low as possible. Minimizing Δu the is predominant factor in the optimization procedure is replicated at every sampling instance [19,20].

Suggested controller's main goal is to dampen the wear stress and enable the mechanism operation in the least power tradeoff state [21]. The goals are to decrease the blade root bending moments without sacrificing power and ii) boost the immediate power output. The active individual pitch angle is the cost function J engaged in fulfilling the goal variables.

Mathematical replication of the linearized MPC controller for an operating point of 4 m/s wind speed is shown below.

$$A = \begin{pmatrix} -0.02 & -36.62 & -18.90 & -32.09 & 3.25 & -0.76 & 0.00 & 0.00 \\ 0.00 & -1.90 & 0.98 & 0.00 & -0.17 & -0.01 & 0.00 & 0.00 \\ 0.01 & 11.72 & -2.63 & 0.00 & -31.60 & 22.40 & 0.00 & 0.00 \\ 0.00 & 0.00 & 1.00 & 0.00 & 0.00 & 0.00 & 0.00 & 0.00 \\ 0.00 & 0.00 & 0.00 & 0.00 & -30.00 & 0.00 & 0.00 & 0.00 \\ 0.00 & 0.00 & 0.00 & 0.00 & 0.00 & -30.00 & 0.00 & 0.00 \\ 0.00 & -1.00 & 0.00 & 0.00 & 0.00 & 0.00 & -0.01 & 0.00 \\ 0.00 & 0.00 & 0.00 & -1.00 & 0.00 & 0.00 & 0.00 & -0.01 \end{pmatrix}$$

$$B = \begin{pmatrix} 0.00 & 0.00 \\ 0.00 & 0.00 \\ 0.00 & 0.00 \\ 0.00 & 0.00 \\ 0.00 & 0.00 \\ 0.00 & 0.00 \\ 1.00 & 0.00 \\ 0.00 & 1.00 \end{pmatrix}$$

$$C = \begin{pmatrix} 0.00 & -0.01 & 0.00 & 0.00 & 0.00 & 0.00 & 1.00 & 0.00 \\ 0.00 & 0.00 & 0.00 & -0.01 & 0.00 & 0.00 & 0.00 & 1.00 \\ 0.00 & 0.02 & 0.00 & 0.00 & -0.03 & 0.02 & 0.00 & 0.00 \\ 0.00 & 0.01 & 0.00 & 0.00 & -0.03 & 0.02 & 0.00 & 0.00 \end{pmatrix}$$

4. Simulation outcomes

The NREL FAST is a simulation software for assessment recognized by several specifications such as IEEE, IEC, and others. The DOFs for the Blade and Generator activities are chosen. Table 1 shows the DOF that was chosen. The suggested controller is integrated remotely through the MATLAB connector, and the simulation data is acquired instantly. Fig. 1 depicts the architectural framework of the design. The NREL's TurbSim program, and the Von Karman turbulence model were used.

Table 1. DOFs enabled in simulation model FAST.

Components	Number of DOFs	Fatigue variable	Number of states
Blades	2	BRBM (flap)	6
	1	BRBM (Edge)	2
Nacelle	1	Yaw angle	1
Drive train	1	Drivetrain dynamics	1
Generator	1	Generator	1
Tower	2	Tower deflections	2
	2	Tower deflections (side-to-side bending mode DOF)	2

Simulation outcomes are shown in Figs. 2 and 3.
Fig. 4 depicts the TTM created on the Blade framework as a result of the distorted wind field.

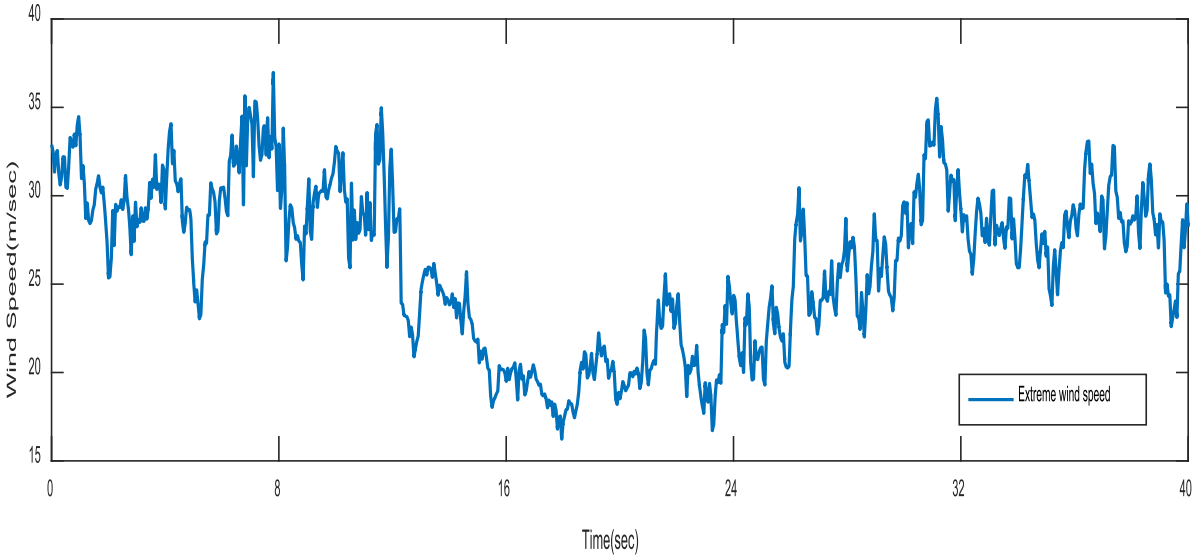

Fig. 2. TurbSim simulated stochastic wind field.

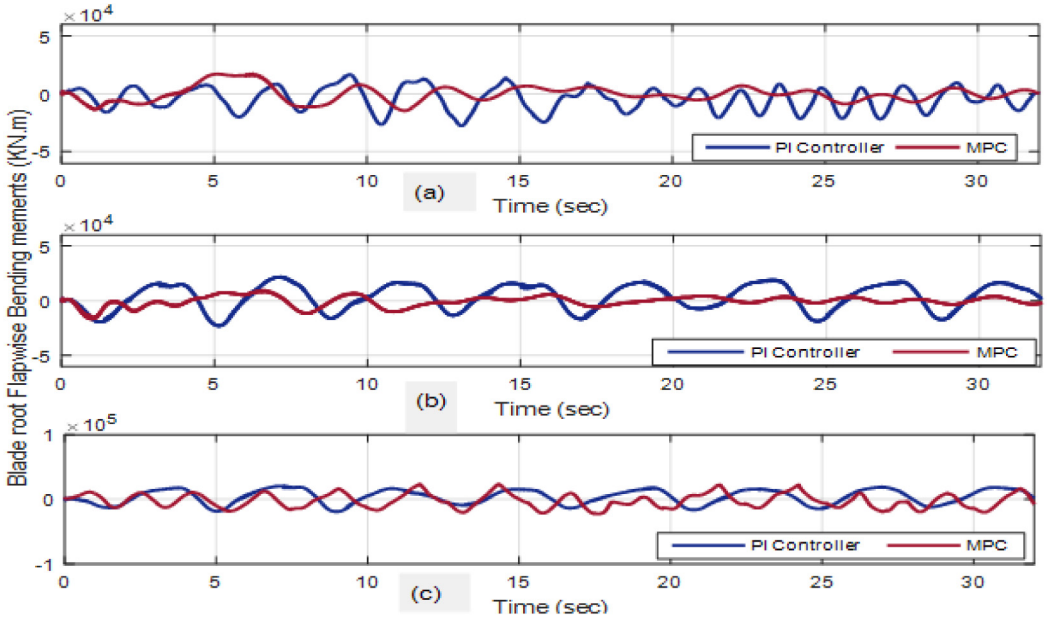

Fig. 3. Flap-wise BRBM of individual blades.

5. Fatigue life analysis

The fatigue existence study is performed using the NREL FAST wind turbine yield responsiveness involving different controller operations. The NREL's MLife program will be utilized to calculate the Lifetime DEL. Depending on this computation, the Lifetime fatigue stress, as well as component lifetime estimate, may be performed [22–31]. Figs. 5, 6, and 7 illustrate a histogram contrasting the fatigue life metrics of several controllers to the suggested controller. Table 2 contains a synopsis of the lifetime assessment (see Fig. 8).

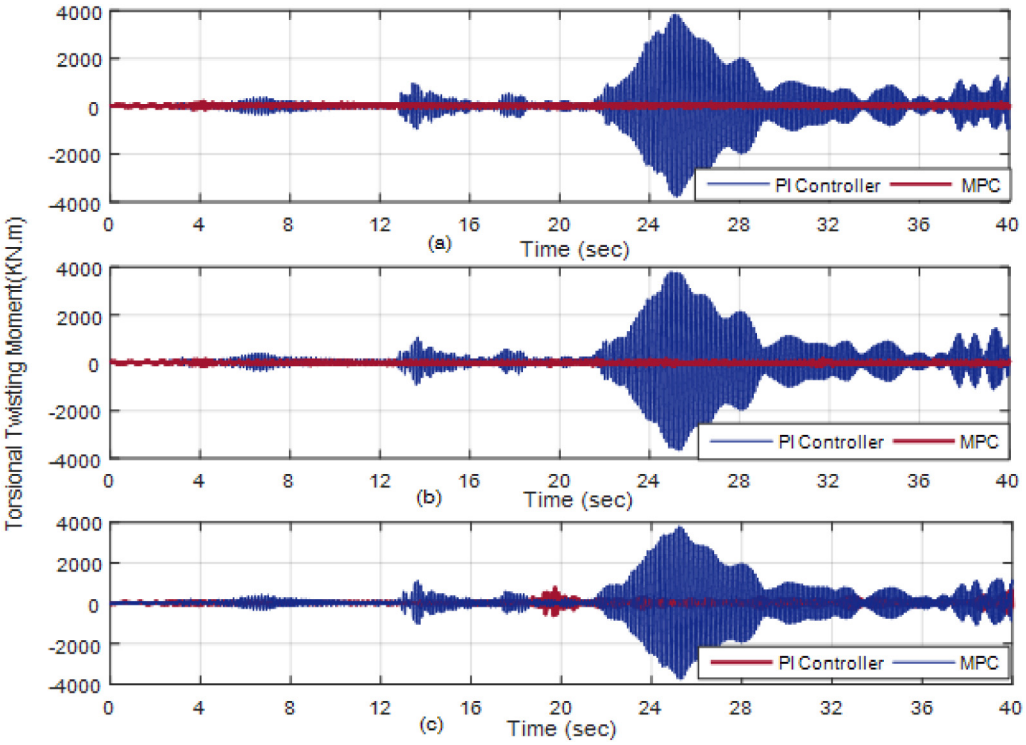

Fig. 4. TTM of 3 blades.

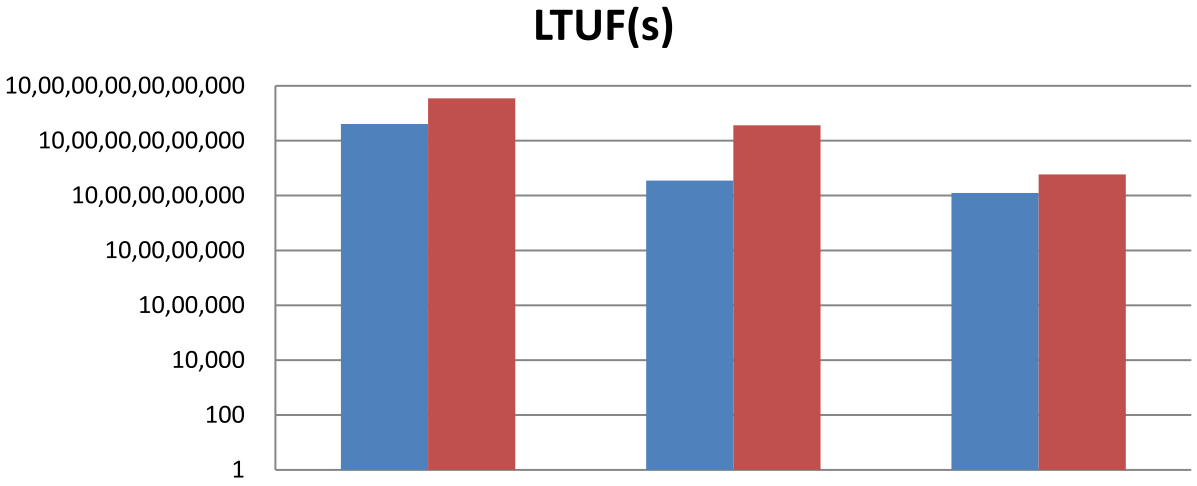

Fig. 5. Representation of LTUF.

6. Conclusion

Suggested controller successfully controls the fatigue stress reduction on the blade structure. The MPC controller's inherent capacity to foresee the forthcoming system behavior and create the controlling response within the defined operational horizon enables effectiveness in mitigating fatigue stress. The findings of the lifetime study indicate that the suggested control logic outperforms the conventional controllers. The suggested controller is 40 percent highly effective compared to the PI controller and 30 percent better compared with the LQG-based controller

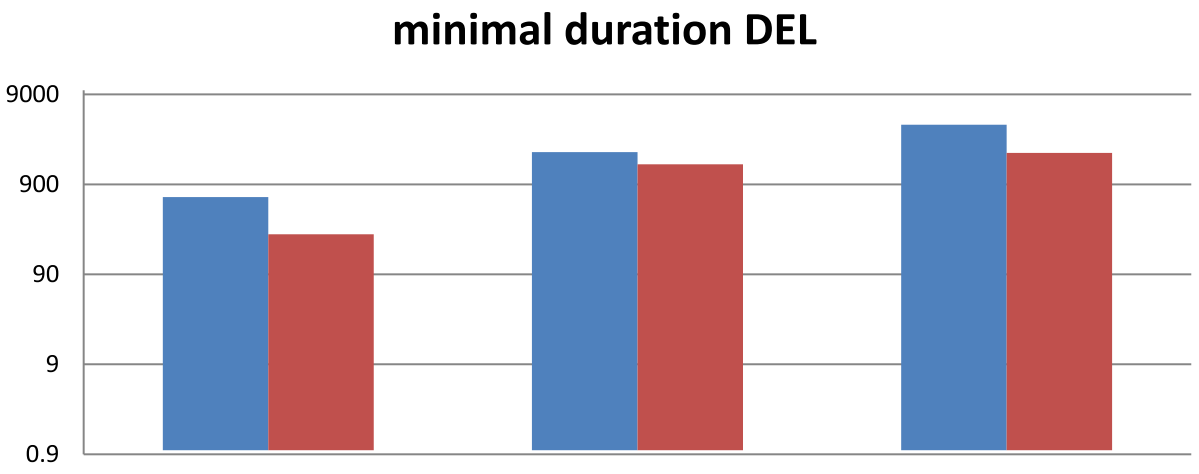

Fig. 6. Representation of MDDEL.

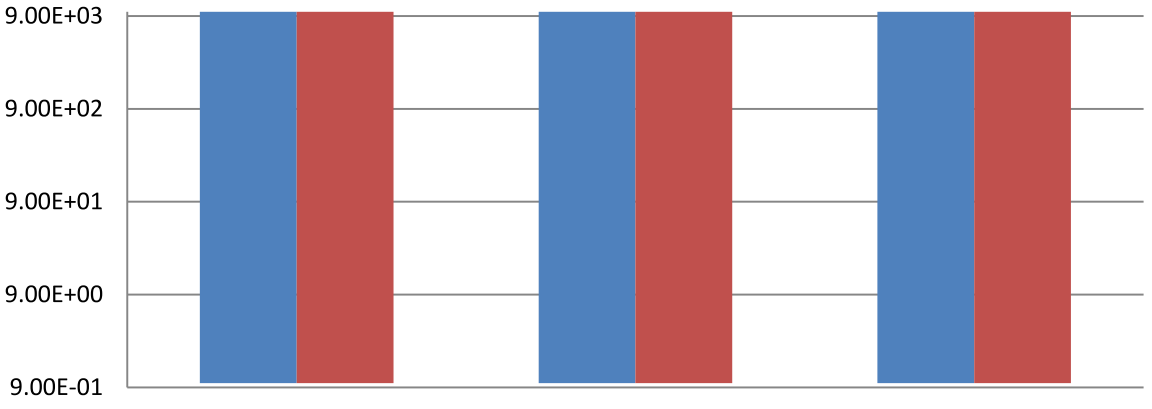

Fig. 7. Lifetime DEL representation.

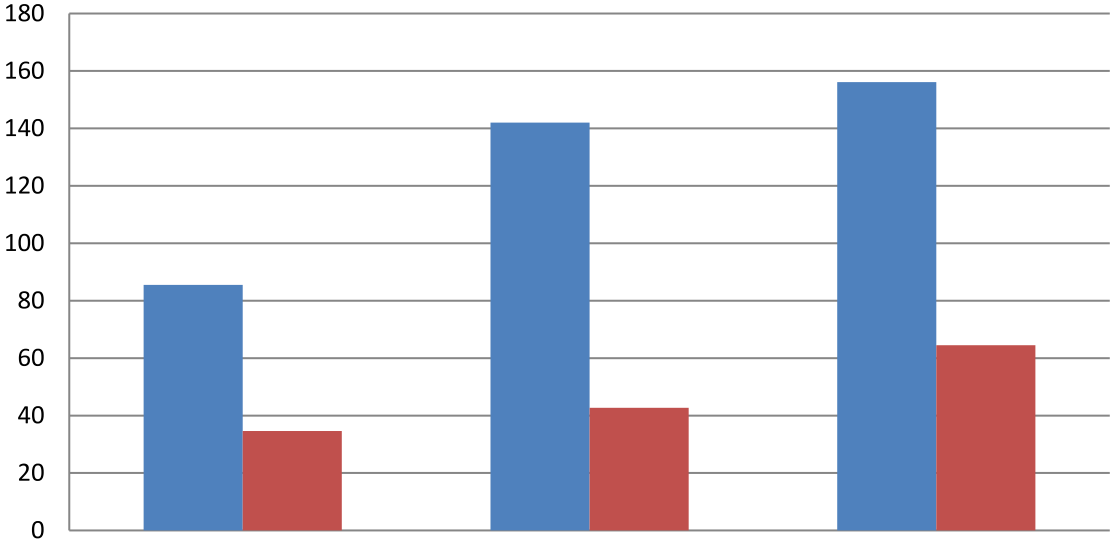

Fig. 8. Depiction of controller variations.

Table 2. Lifetime investigation outcome synopsis.

LTAP	FLP	PIC (%)	LQC (%)	MPC (%)
LEV	Summit fore-aft shearing force	78.56	54.296	31.37
	Summit side shearing	90.09	44.88	31.73
MV	Summit frontal-rear shearing	72.061	50.252	35.523
	Summit side shearing	94.33	47.14	20.30

in terms of life duration fatigue degradation. Therefore, the suggested controller for active flow regulation technology is found to extend the lifespan of the wind turbine.

Declaration of competing interest

The authors declare that they have no known competing financial interests or personal relationships that could have appeared to influence the work reported in this paper.

Data availability

The data that has been used is confidential.

References

[1] Burton T, Sharpe D, Jenkins N, Bossanyi E. Wind energy handbook. John Wiley & Sons Ltd; 2001.
[2] Lasheen A, Elshafei AL. Wind-turbine collective-pitch control via a fuzzy predictive algorithm. Renew Energy 2016;87:298–306.
[3] Xiao S, Geng H, Yang G. Non-linear pitch control of wind turbines for tower load reduction. IET Renew Power Gener 2014;8(7):786–94.
[4] Jang YJ, Choi CW, Lee JH, Kang KW. Development of fatigue life prediction method and effect of 10-minute mean wind speed distribution on fatigue life of small wind turbine composite blade. Renew Energy 2015;79:187–98.
[5] Petrovi V, Jelavi M, Baoti M. Advanced control algorithms for reduction of wind turbine structural loads. Renew Energy 2015;76:418–31.
[6] Zhang Wenguang, Bai Xuejian, et al. Optimization of sizing parameters and multi-objective control of trailing edge flaps on a smart rotor. Renew Energy 2018;129:75–91, Elsevier.
[7] Andersen PB. Advanced load alleviation for wind turbines using adaptive trailing edge flaps: sensor and control (Ph.D. thesis), 2010, case number: 274-05-0398.
[8] Chen D, Liu S, Xiaoyi M. Modeling, nonlinear dynamical analysis of a novel power system with random wind power and it's control. Energy 2013;53:139–46.
[9] Rahman M, Ong ZC, Chong WT, Julai S, Khoo SY. Performance enhancement of wind turbine systems with vibration control: A review. Renew Sustain Energy Rev 2015;51:43–54.
[10] Teng L, Wang Y, Cai W, Li H. Fuzzy model predictive control of discrete-time systems with time-varying delay and disturbances. IEEE Trans Fuzzy Syst 2018;26(3):1192–206.
[11] Runfan Z, Diyi C, Wei Y, Duoduo B, Xiaoyi M. Non-linear fuzzy predictive control of hydroelectric system. IET Gener Transm Distrib 2017;11(8):1966–75.
[12] Kumar PM, Saminathan R, Tharwan M, Hadidi H, Stalin P, Kumaresan G, Ram S, Rinawa ML, Saravanakumar PT, Karthikeyan K, Gebreyohannes DT. Study on sintered wick heat pipe (SWHP) with CuO nanofluids under different orientation. J Nanomater 2022. http://dx.doi.org/10.1155/2022/7158228.
[13] Chen ZJ, Stol KA, Mace BR. Wind turbine blade optimisation with individual pitch and trailing edge flap control. Renew Energy 2017;148:964–74, Elsevier.
[14] Zhang Y, Cheng M, Chen Z. Load mitigation of unbalanced wind turbines using PI-R individual pitch control. IET Renew Power Gener 2015;9(3):262–71.
[15] Senthil Kannan N, Parameshwaran R, Saravanakumar PT, Kumar PM, Rinawa ML. Performance and quality improvement in a foundry industry using fuzzy MCDM and lean methods. Arab J Sci Eng 2022;1–12. http://dx.doi.org/10.1007/s13369-022-06627-6.
[16] Hassan HM, Elshafei AL, Farag WA, Saad MS. A robust LMI-based pitch controller for large wind turbines. Renew Energy 2012;44:63–71.
[17] XingWeia B, FengNg, et al. Aeroelastic load control of large and flexible wind turbines through mechanically driven flaps. J Franklin Inst B 2019;356:7810–35.
[18] Parys Bart PG Van, Ng Bing Feng, Goulart Paul J, Palacios Rafael. Optimal control for load alleviation in wind turbines. American Institute of Aeronautics and Astronautics; 2010, p. 1–12.
[19] Lakshmanpriya C, Kumaravel A, Saravanan M, Kumar PManoj. Selecting the optimal Green supplier and order allocation under linear discount. Math Probl Eng 2022. http://dx.doi.org/10.1155/2022/2453703.
[20] Johnson KE. Adaptive torque control of variable speed wind turbines. NREL Tech. Rep NREL/TP-500-36265, 2004.
[21] Berg JC, Barone MF, Yoder NC. SMART wind turbine rotor: data analysis and conclusions. Sandia report SAND2014-0712, 2014.

[22] Andersen Peter Bjoern, Henriksen Lars, Gaunaa Mac. Deformable trailing edge flaps for modern megawatt wind turbine controllers using strain gauge sensors. Wind Energy 2009;13. Wiley.
[23] Boukhezzar B, Lupu L, Siguerdidjane H, Hand M. Multivariable control strategy for variable speed, variable pitch wind turbines. Renew Energy 2007;32:1273–87.
[24] Dinesh SN, Saminathan R, Patil MM, Baviskar PR, Hadidi H, Vignesh S, Kumar PM. Investigating the single pass baffled solar air heater (SAH) with an organic PCM (OPCM). Mater Today Proc 2022. http://dx.doi.org/10.1016/j.matpr.2022.03.216.
[25] Fischer A, Madsen HA. Investigation of the theoretical load alleviation potential using trailing edge flaps controlled by inflow data. Wind Energy 2015;19. Wiley.
[26] Rafiee Roham, Reza Mohammad, Hashemi-Taheri. Failure analysis of a composite wind turbine blade at the adhesive joint of the trailing edge. Eng Fail Anal 2021;121.
[27] Thakur Shilpa, Abhinav KA, Saha Nilanjan. Stochastic response reduction on offshore wind turbines due to flaps including soil effects. Soil Dyn Earthq Eng 2018;114:174–85, Elsevier.
[28] Yang W, Feng G, Zhang T. Robust model predictive control for discrete-time takagi–sugeno fuzzy systems with structured uncertainties and persistent disturbances. IEEE Trans Fuzzy Syst 2014;22(5):1213–28.
[29] Zhu Haitian, Hao Wenxing, et al. Effect of flow-deflecting-gap blade on aerodynamic characteristic of vertical axis wind turbines. Renew Energy 2020;158:370–87, Elsevier.
[30] Zhuang Chen, Yang Gang, et al. Effect of morphed trailing-edge flap on aerodynamic load control for a wind turbine blade section. Renew Energy 2017;103:750–65, Elsevier.
[31] Ning SA. Airfoilprep.py documentation. NREL Technical Report NREL/TP-5000-58817, 2013.